Applied Catalysis A: General 391 (2011) 225–233

Contents lists available at ScienceDirect

Applied Catalysis A: General

journal homepage: www.elsevier.com/locate/apcata

Nitridation of BaO supported on mesoporous materials: Basicity characterization and catalytic properties

Guangjun Wu[a,b], Shaoliang Jiang[c], Landong Li[a], Naijia Guan[a,*]

[a] The Key Laboratory of Functional Polymer Materials, College of Chemistry, Nankai University, Tianjin 300071, PR China
[b] College of Physics, Nankai University, Tianjin 300071, PR China
[c] Research and Development Base of Catalytic Hydrogenation, Zhejiang University of Technology, Hangzhou 310032, PR China

ARTICLE INFO

Article history:
Received 25 February 2010
Received in revised form 11 May 2010
Accepted 19 July 2010
Available online 27 July 2010

Keywords:
BaO
Mesoporous materials
Nitridation
Basicity
Base-catalyzed reactions

ABSTRACT

Nitridation has drawn much attention as a novel method to prepare solid base materials. In the present work, nitridation was employed to improve the basic property of BaO supported on mesoporous materials. Ba_2SiO_4 and $Ba_4Si_6O_{16}$ basic species were formed after BaO loading on MCM-41 and SBA-15, respectively while only Ba_2SiO_4 species were observed both on MCM-41 and SBA-15 after nitridation. Basic species, bridging –NH– groups, were introduced into the framework of BaO-MCM-41/SBA-15 by nitridation with the mesoporous structure preserved. The surface basic property of obtained samples was analyzed by IR spectra using $CDCl_3$ and CO_2 as probe molecules and XPS. The enhancement in the surface basicity was observed after nitridation. Compared with BaO-MCM-41/SBA-15, the N-incorporated materials with stronger basicity exhibited higher activities in Knoevenagel condensation and the conversion of 2-propanol.

1. Introduction

Solid base materials have attracted more and more interest in the past decades, due to their potential application as environmentally friendly catalysts in a number of important industrial reactions, especially for fine chemical synthesis [1]. Molecular sieves (MS), including zeolites and mesoporous materials, are families of solids with unique structures and high surface areas, which can serve as support materials for the solid base catalysts. Conventionally, basic MS can be prepared *via* ion exchange with alkali metal cations [2–4], incorporation of alkaline earth metal oxides [3,4], impregnation with alkali metal ions/basic salts [5,6], deposition of basic guests in the cavities [7], isomorphous substitution of silicon by germanium in the framework [8], and grafting of organic functional moieties onto the pore walls [9–11].

Recently, nitridation at elevated temperature is adopted as a completely different approach to prepare basic MS, in which O atoms in the framework of MS are partially substituted by N atoms (N-incorporated MS) and bridging –NH– basic groups are formed. Compared with basic MS prepared from conventional methods, high specific surface areas and porous structures can be well preserved after nitridation under proper conditions. Up to now, various types of N-incorporated MS (MS-N), such as FSM-16 [12], MCM-48 [13,14], SBA-15 [15,16], MCM-41 [17,18], NaY [19–23], SAPO-11 [24], ZSM-5 [25–27], SAPO-34 [28], Beta [29] and B-SSZ-13 [30] have been successfully prepared. As expected, the basic property of MS is improved after nitridation, and all MS-N materials exhibit good activity in Knoevenagel condensation, a typical probe reaction catalyzed by basic materials. Unfortunately, none of the above-mentioned MS-N has been reported to be used for industrial application. Theoretic studies have demonstrated that N-incorporated zeolites can also be considered as bifunctional acid–base catalysts [31,32]. So in some cases, nitridation is also employed as an efficient modified method to adjust the surface acidity of MS [26]. That is, although the nitrogen content of MS-N can reach as high as 25%, which means over 60% of O atoms in the framework has been substituted by N atoms [17], the basicity of MS-N is still not strong enough for most base-catalyzed reactions, except the basic probe reaction. Moreover, detailed characterizations are highly desired to explore the chemical nature of the basic sites generated by nitridation [33].

In the present work, a new method to prepare basic MS with strong basicity is developed by the combination of nitridation and impregnation of alkaline oxides. BaO is firstly loaded on mesoporous materials by impregnation and the obtained materials are subsequently nitridized at elevated temperatures. MCM-41 and SBA-15 are selected as mesoporous support, due to their stable mesoporous structure and large surface areas. Various characterization methods, including XRD, low temperature N_2 adsorption, TEM, XPS, and IR spectroscopy are employed to analyze the

* Corresponding author. Tel.: +86 22 23509140; fax: +86 22 23509140.
E-mail address: guannj@nankai.edu.cn (N. Guan).

0926-860X/$ – see front matter © 2010 Elsevier B.V. All rights reserved.
doi:10.1016/j.apcata.2010.07.033

physical–chemical properties of as-prepared materials. Especially, $CDCl_3$ and CO_2 are used as probe molecules for IR analysis to test the basic strength and density of as-prepared materials. In addition to Knoevenagel condensation, the conversion of 2-propanol, the most popular model reaction for the evaluation of both surface acidic and basic properties of catalysts [34], is employed to test the acidic/basic properties of as-prepared materials. However, as reviewed by Busca [35], pure basicity on solids actually does not exist, but acid–base couples with predominant basicity are active in adsorption, catalysis, and surface reactivity. So, we will focus on the basicity of as-prepared samples in this study.

2. Experiment

2.1. Sample preparation

MCM-41 and SBA-15 were synthesized according to the literature reports [36,37].

BaO-MCM-41/SBA-15: 6.386 g $Ba(Ac)_2$ (AR) was dissolved into 100 ml distilled water and then 1.0 g MCM-41/SBA-15 was added under stirring. After evaporated at 50 °C under vacuum condition for 3 h, the sample was dried at 70 °C for 12 h and then calcined at 500 °C for 4 h. The Ba loadings on BaO-MCM-41 and BaO-SBA-15 are 18.0 and 16.0 wt%, respectively.

Nitridation: 0.4 g BaO-MCM-41/SBA-15 was placed in a quartz boat and treated with NH_3 flow (99%) at 700 °C in a quartz tube furnace. The NH_3 flow rate is 400 ml/min and the heating rate is 2 °C/min. After treating for 10 h, the N-incorporated BaO-MCM-41 (denoted as BaO-MCM-41N) and BaO-SBA-15 (denoted as BaO-SBA-15N) were cooled down to room temperature (RT) and further treated in vacuum at 120 °C for 4 h to remove the adsorbed NH_3. The nitrogen contents of BaO-MCM-41N and BaO-SBA-15N are 2.86 and 4.68 wt%, respectively.

2.2. Sample characterization

Total nitrogen content of as-synthesized samples was determined by CNH elemental analysis on an Elementar Vario EL analyzer.

The Ba loading in BaO-MCM-41/SBA-15 was analyzed by ICP (IRIS Advantage, TJA solution). The samples were dissolved into a mixture acid of HCl and HF to get a clear solution and then diluted before ICP test.

Powder X-ray diffraction patterns were collected on a D/Max-2500 powder diffractometer (36 kV and 20 mA) using Cu Kα (k = 1.54178 å) radiation. Small-angle X-ray scattering (SAXS) patterns were collected on a C79298-A3244 small-angle diffractometer.

Nitrogen adsorption/desorption measurements were performed at 77 K using a NOVA 1000e apparatus (Quantachrome Co.) after outgassing the samples for 12 h at 200 °C under vacuum.

Transmission electron microscopy (TEM) images were taken on a Philips Tecnai G^2 20 S-TWIN electron microscope at an accelerate voltage of 200 kV. A few drops of alcohol suspension containing the sample were placed on a carbon-coated copper grid, followed by evaporation at ambient temperature.

The X-ray photoelectron spectroscopy (XPS) measurements were acquired using a PHI 5300 ESCA XPS spectrometer with monochromatic Mg Kα excitation, and all the bonding energies were calibrated to the C 1s peak at 284.6 eV of the surface adventitious carbon.

IR spectra of the samples were recorded in transmission prior to and after adsorption of probe molecules on a Bruker IFS-66 spectrometer at a spectral resolution of 2 cm^{-1} and accumulation of 128 scans. The IR cell was purpose-made for recording spectra in situ at RT or certain high temperatures. The cell was connected to a vacuum adsorption system with a base pressure below 10^{-3} Pa. Self-supporting wafers of the samples were thermally treated in an oxygen flow in the cell at 300 °C for 2 h or 490 °C for 1 h followed by evacuation at the same temperature to remove contaminations and adsorbed water. After recording the background spectra, the adsorption of various probe molecules was detected by their vibrational spectra in the adsorbed state.

2.3. Catalytic test

The as-prepared solid base materials were tested as catalysts for Knoevenagel condensation and the conversion of 2-propanol.

Knoevenagel condensation: Benzaldehyde (20 mmol), malononitrile (20 mmol) and 40 ml of toluene were added into a round bottom flask which was equipped with a magnetic stirrer and a reflux condenser and immersed in a thermostatic oil bath. Once the mixture reached 80 °C, 0.2 g catalyst was added into the flask. Small liquid samples of 0.5 μl were then periodically withdrawn from the reaction mixture with a syringe and analyzed in a SP-502 gas chromatograph equipped with a FID and a 0.20 mm × 50 m FFAP capillary column by corrected peak area normalization.

Conversion of 2-propanol: The reaction was carried out on a fixed-bed microreactor at atmospheric pressure. About 0.2 g of the catalyst (mesh of 20–40) was placed in the isothermal region of the reactor. After the reactor was heated to the desired temperature for 1 h, the reactant of isopropanol was fed into the reactor by a syringe infusion pump (0.4 ml/h) with N_2 as the carrier gas (20 ml/min). After reaction for 1 h, the product was analyzed in a SP-502 gas chromatograph equipped with a FID and a 4 mm × 3 m packed column by corrected peak area normalization.

3. Results and discussion

3.1. Structural property

Fig. 1 shows the small-angle XRD patterns of BaO-MCM-41 and SAXS patterns of BaO-SBA-15 before and after nitridation. Qualitatively, the typical highly ordered mesoporous structures are preserved in the BaO-MCM-41/SBA-15 and BaO-MCM-41N/SBA-15N samples. However, compared to parent MCM-41 and SBA-15, the intensities of peaks decrease after BaO loading and nitridation. Meanwhile, the (1 0 0) peaks of MCM-41/SBA-15 gradually shifts to higher 2θ values. This indicates the shrinkage of unit cell and/or mesopores, which is caused by BaO loading and nitridation at elevated temperature. This can also be indicated by the varieties of porous parameters and surface areas determined by N_2 sorption measurements, as summarized in Table 1. After loading of BaO, as the surface is partially covered and some mesopores are blocked by BaO, the surface area decreases obviously, so do the average pore size and pore volume. Typically, the surface area and pore volume decrease by 62% and 78% for BaO-MCM-41, and 61% and

Table 1
Porous parameters via N_2 adsorption on BaO-MCM-41/SBA-15 before and after nitridation.[a].

Samples	Specific surface area ($m^2\ g^{-1}$)	Average pore size (nm)	Pore volume ($cm^3\ g^{-1}$)
MCM-41	1032	3.32	1.49
BaO-MCM-41	400	2.90	0.326
BaO-MCM-41N	232	2.77	0.233
SBA-15	607	7.3	0.378
BaO-SBA-15	235	7.2	0.169
BaO-SBA-15N	183	6.6	0.141

[a] The parameters were calculated by DFT method.

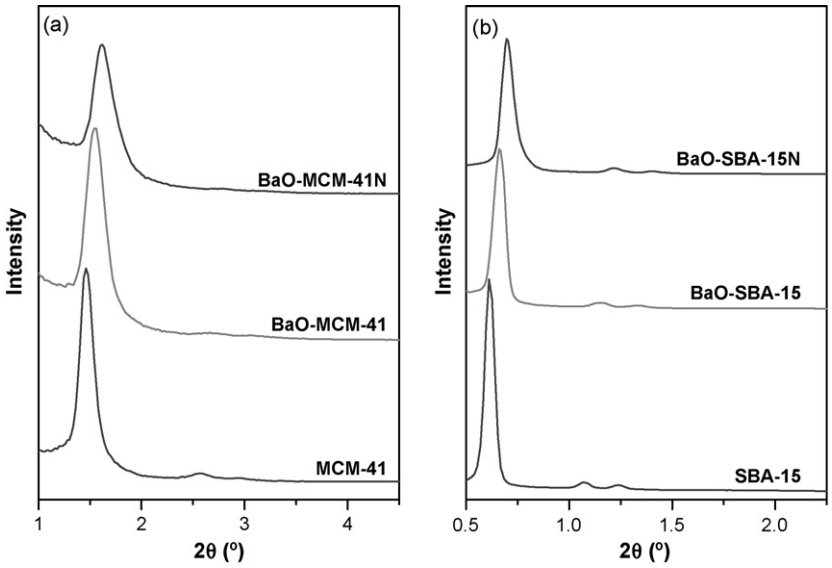

Fig. 1. Small-angle XRD patterns of BaO-MCM-41 (a) and SAXS patterns of BaO-SBA-15 (b) before and after nitridation.

41% for BaO-SBA-15, respectively. Nitridation also shows negative effect on the porous structure and mild decrease of surface area is observed. Probably, this is due to the shrinkage of unit cell and/or mesopores at elevated temperature, as supported by the decrease of the average pore size and the pore volume. Nevertheless, highly ordered mesoporous structures are still well preserved in the final products of BaO-MCM-41N and BaO-SBA-15N, as supported also by the TEM images in Fig. 2.

It is known that impregnation always leads to poor dispersion of the loaded phase, a modified impregnation method [38] was used here for BaO loading and the surface species were characterized by wide-angle XRD patterns, as shown in Fig. 3. It is seen that no peak attributed to BaO species can be observed on XRD patterns of BaO-MCM-41 or BaO-SBA-15 after BaO loading. For BaO-MCM-41 before and after nitridation, peaks at 26.1°, 29.5°, 30.4°, and 30.7° are observed, which can be attributed to Ba_2SiO_4 species [38]. It indicates that BaO after loading reacts with the surface of MCM-41 and new species Ba_2SiO_4 are formed. For BaO-SBA-15, peaks at 23.8°, 24.2°, 24.8°, 26.0°, and 27.6° are observed after BaO loading, which can be attributed to $Ba_4Si_6O_{16}$ species (JCPDS, 83-1442). However, after nitridation, the $Ba_4Si_6O_{16}$ species transform into Ba_2SiO_4 species. It means that the basic species are Ba_2SiO_4 on BaO-MCM-41 and $Ba_4Si_6O_{16}$ on BaO-SBA-15, while after nitridation, the basic species on both BaO-MCM-41N and BaO-SBA-15N are Ba_2SiO_4. It indicates that BaO shows different interactions with the surface of MCM-41 and SBA-15. Therefore, the basicity of BaO-MCM-41 before and after nitridation is different to BaO-SBA-15 before and after nitridation, as proved by the results from following IR characterizations and catalytic tests.

IR characterization can efficiently distinguish different NH_x groups formed on the surface by nitridation, and thus can be used to confirm the substitution of O atoms by N atoms [23,27]. So here, IR spectroscopy is used to determine the surface groups formed by nitridation. The samples are pretreated under vacuum condition at 573 K for 1 h to diminish the contributions of adsorbed water and other contaminations. As shown in Fig. 4, the BaO-MCM-41/SBA-15 presents a strong band at 3700 cm^{-1} which can be attributed to the O–H vibration of Si–OH groups. After nitridation, two new bands at 2173 and 3386 cm^{-1} appear. The former band has not been previously reported on N-incorporated porous materials. According to the literatures [39], this band is assigned to vibration of Si–H groups. It suggests that the loading of BaO may have some effect on the nitridation process and results in the formation of Si–H groups on the surface after nitridation. The latter bands, based on

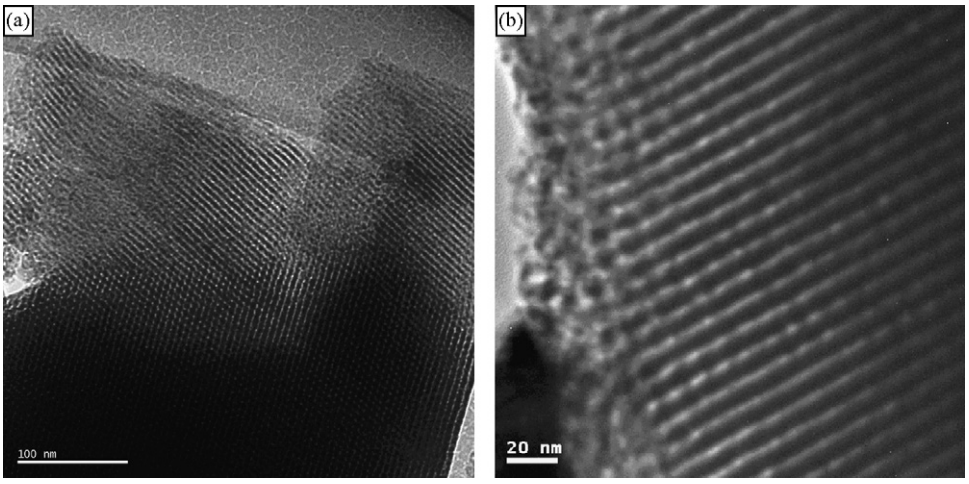

Fig. 2. TEM images of BaO-MCM-41N (a) and BaO-SBA-15N (b).

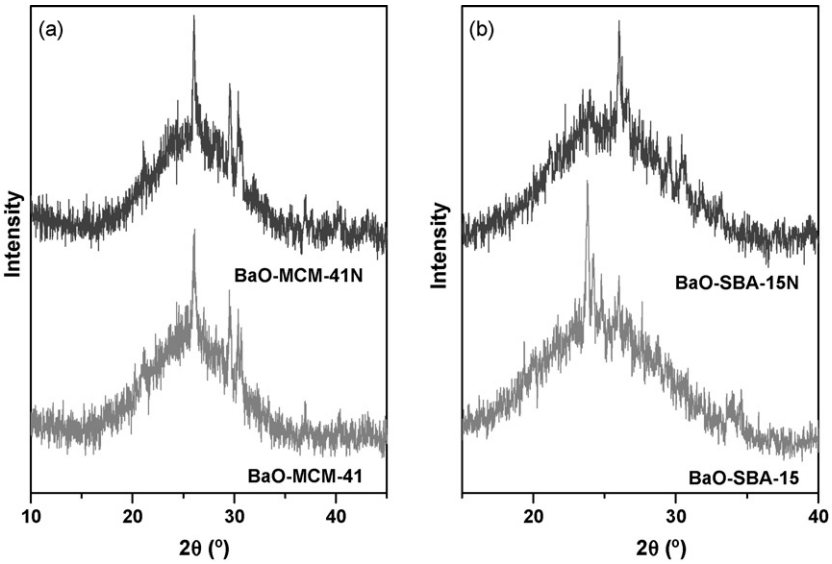

Fig. 3. Wide-angle XRD patters of BaO-MCM-41 (a) and BaO-SBA-15 (b) before and after nitridation.

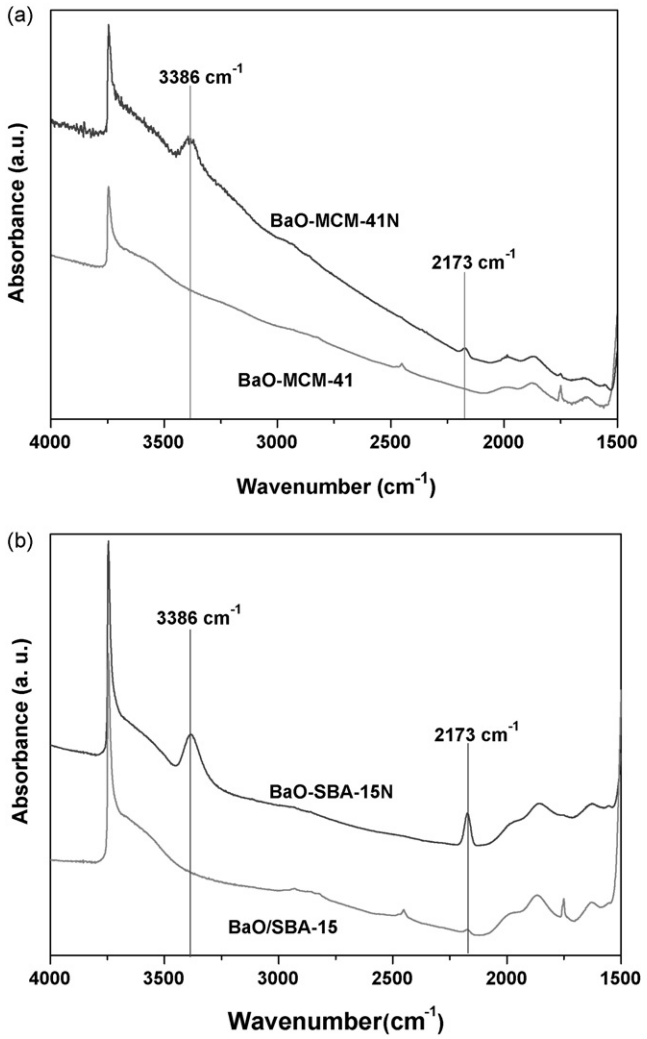

Fig. 4. IR spectra of BaO-MCM-41 (a) and BaO-SBA-15 (b) before and after nitridation.

the literature reports [16–18,27], is attributed to N–H asymmetric vibration of bridging Si–NH–Si groups, the appearance of which can unambiguously confirm the substitution of oxygen by nitrogen. It should be noted that the bridging –NH– groups are always considered as the basic center of MS-N. Combined with the results of wide-angle XRD characterizations, it indicates that two basic centers are formed after nitridation. One is Ba_2SiO_4 species formed by BaO loading and nitridation, another one is bridging –NH– group formed by nitridation.

3.2. Basic property

3.2.1. Binding energy of O 1s

XPS spectroscopy is considered as a technique to provide direct evidence of basic surface sites, as the position of the O 1s binding energy XPS peak is correlated to the surface basicity of metal oxides [35]. Fig. 5 shows the O 1s binding energy XPS peak of BaO-MCM-41/SBA-15 before and after nitridation. It can be seen that the binding energies of O 1s for BaO-MCM-41 and BaO-SBA-15 are 532.9 and 532.7 eV, respectively. After nitridation, the binding energies of O 1s for BaO-MCM-41N and BaO-SBA-15N decrease to 532.6 and 532.4 eV, respectively. This indicated that the Lewis basicity of the surface increases after nitridation [38].

3.2.2. IR spectra of $CDCl_3$ adsorption

$CDCl_3$ is used as a probe molecule to characterize the type and strength of surface basic sites of as-prepared BaO-MCM-41N and BaO-SBA-15N. It is known that $CDCl_3$ is a protonic acid able to form D complexes with the basic center. Also, it is a weak base (Cl), which is associated with the weak acid character of the molecule. Its interaction with aptotic or protonic surface centers is negligible. Furthermore, the ν_{CD} bands, the vibration of interest, are situated between 2250 and 2180 cm^{-1}, which is particularly free of perturbation in the IR spectra of samples. Therefore, the complexes of the probes with the basic sites can be clearly distinguished from the bands of the surface OH groups and can be clearly recognized [40,41].

The IR spectra of $CDCl_3$ on BaO-MCM-41/SBA-15 before and after nitridation are shown in Fig. 6. The dominated bands at 2264 cm^{-1} attributed to ν_{CD} from physical absorbed $CDCl_3$ are observed in all samples. A broad shoulder band at 2224 cm^{-1} attributed to ν_{CD} from $CDCl_3$ interaction with basic sites is also observed. Higher

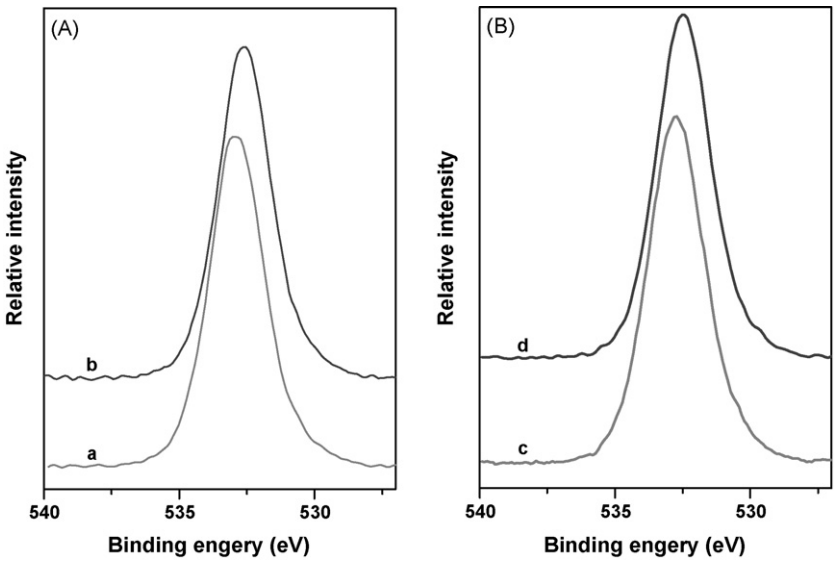

Fig. 5. XPS spectra of BaO-MCM-41 (A) and BaO-SBA-15 (B) before and after nitridation focusing on O 1s peak. (a) BaO-MCM-41, (b) BaO-MCM-41N, (c) BaO-SBA-15, (d) BaO-SBA-15N.

pretreated temperature can make the surface neat and thus the shoulder band becomes clearer. After nitridation, the shoulder band at 2224 cm^{-1} slightly decreases, while the bands at 2180 cm^{-1} for BaO-MCM-41N and 2190 cm^{-1} for BaO-SBA-15N increase. It indicates that the surface basicity is modified by nitridation and new basic sites are formed. A feature to note is that the new basic sites on BaO-SBA-15N are much more than that on BaO-MCM-41N. This should be due to the higher N content of BaO-SBA-15N (4.68 wt%) than that of BaO-MCM-41N (2.86 wt%).

It has been reported that the strength of the basic sites can be distinguished by the wavenumber of ν_{CD} bands: the lower wavenumber of the ν_{CD} bands, the stronger of the basic sites [42]. Therefore, the strength of each basic site can be compared by their $\Delta\nu_{CD}$ shift ($\Delta\nu_{CD} = [\nu_{CD}]_{gas} - [\nu_{CD}]_{adsorbed}$). Furthermore, the p$K_a$ and proton affinity (PA) values, which can be used as a measurement of the basic strength, can be also estimated by the $\Delta\nu_{CD}$ [40,42,43]. Table 2 presents the $\Delta\nu_{CD}$, pK_a and PA values for BaO-MCM-41/SBA-15 before and after nitridation. Obviously, basic sites

Table 2
Estimated pK_a and proton affinity (PA) values for BaO-MCM-41/SBA-15 before and after nitridation.

ν_{CD} (cm^{-1})	$\Delta\nu_{CD}$ (cm^{-1})	pK_a[a]	PA[a] (kJ/mol)
2224	41	+8	904
2210	55	+10	926
2190	75	+14	950
2180	85	+15	960

[a] The values were estimated from Refs. [40,42,43]. $\Delta\nu_{CD} = [\nu_{CD}]_{gas} - [\nu_{CD}]_{adsorbed}$, $[\nu_{CD}]_{gas}$=2265 cm^{-1}, PA = (3.54 + log[$\Delta\nu_{CD}$])/0.0057.

with certain strength (pK_a is main from +8 to +10) exist on the surface of BaO-MCM-41/SBA-15. The new basic sites formed by nitridation show stronger strength (pK_a = +14 to +15). It is theoretically demonstrated that bridging –NH– groups, which are formed by nitridation, can be considered as strong Lewis basic centers [44]. So the new stronger basic sites can be attributed to bridging –NH– groups formed by nitridation and/or O atoms, the basic strength of

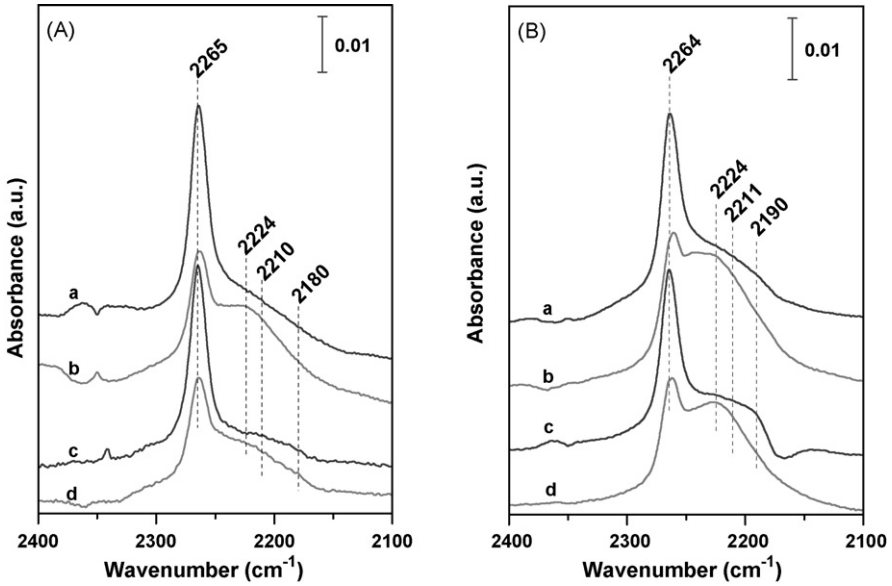

Fig. 6. IR spectra of $CDCl_3$ on BaO-MCM-41 (A) and BaO-SBA-15 (B) before (a and b) and after nitridation (c and d). The samples were evacuated at 300 °C for 2 h (a and c) and 490 °C for 1 h (b and d) before adsorption at RT of $CDCl_3$ (30 hpa).

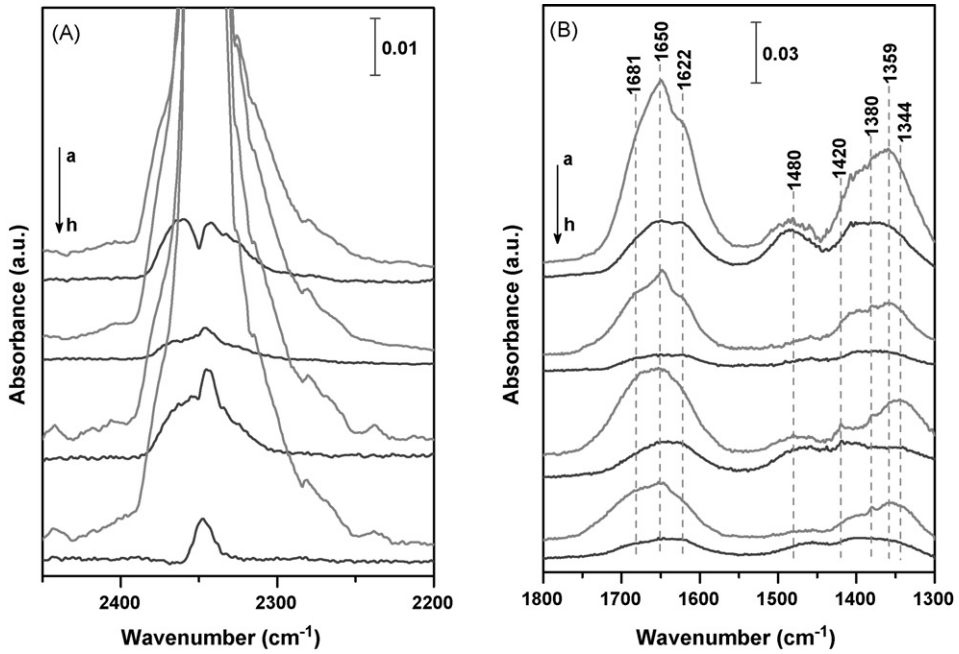

Fig. 7. IR spectra of (a) 21 hpa CO_2 on BaO-MCM-41 evacuated at 300 °C for 2 h, (b) following evacuated at RT for 1 h, (c) 20 hpa CO_2 on BaO-MCM-41 evacuated at 490 °C for 1 h, (d) following evacuated at RT for 1 h, (e) 21.3 hpa CO_2 on BaO-MCM-41N evacuated at 300 °C for 2 h, (f) following evacuated at RT for 1 h, (g) 21.3 hpa CO_2 on BaO-MCM-41N evacuated at 490 °C for 1 h, and (h) following evacuated at RT for 1 h.

which is enhanced by nitridation, as indicated by the result of XPS characterization. Moreover, the amount of basic sites on BaO-SBA-15N is higher than that on BaO-MCM-41.

3.2.3. IR spectra of CO_2 adsorption

CO_2 is an amphoteric molecule and frequently used to probe both the surface basic oxygen and Lewis acid sites of metal oxides and zeolites [45,46]. On Lewis acid sites, CO_2 is adsorbed in a linear configuration and their main IR bands are in range from 2200 to 2400 cm^{-1}. On basic oxygen anion sites, CO_2 is adsorbed to form carbonate-like species, and the main carbonate IR bands are in the range from 1200 to 1700 cm^{-1}. Through different species in the IR spectra, information about surface basic and Lewis acid property can be obtained.

The IR spectra of CO_2 adsorbed on BaO-MCM-41 before and after nitridation are shown in Fig. 7. In the IR region of linear CO_2 adsorption (Fig. 7A), the spectra of all samples (a, c, e, g) are dominated by the very intense band at 2347 cm^{-1}, due to the asymmetric stretching vibration (ν_3 mode) of CO_2 linear adsorbed on Ba^{2+}. Small bands or shoulders are also observed at 2326, 2315, and 2280 cm^{-1}. The former two bands are probably assigned to CO_2 linear adsorbed on less exposed Ba^{2+} cations, and the latter band at 2280 cm^{-1} is assigned to the ν_3 mode of $^{13}CO_2$, the intensity of which is about 100 times lower than that corresponding to the ν_3 mode of $^{12}CO_2$ [47]. After evacuated at RT for 1 h, the intensity of all bands decreases greatly (Fig. 7A), as weak adsorption of CO_2 is removed. Also, the dominated band splits into two bands, one is at 2342 cm^{-1} and another is at 2360–2365 cm^{-1}. The former is attributed to ν_3 mode of CO_2 linear adsorbed on Ba^{2+}, and the latter may be due to a double-coordinated CO_2 molecule and/or CO_2 adsorbed on remanent Na^+ [47] from synthesis process of MCM-41. Furthermore, the band at 2347 cm^{-1} increases after nitridation. This can be observed more clearly when pretreated temperature increases. It indicates that nitridation influences the surface species and thus increases the interaction of CO_2 with basic sites.

In the IR region of carbonate-like species (Fig. 7B), bands at 1681, 1650, 1622, 1480, 1420, 1380, 1359, and 1344 cm^{-1} are observed. There are three species of carbonate after CO_2 adsorbed on basic oxygen sites: unidentate carbonate ($\nu_{as\ O-C-O}$ at 1510–1560 cm^{-1}, and $\nu_{as\ O-C-O}$ at 1360–1400 cm^{-1}), bidentate carbonate ($\nu_{as\ O-C-O}$ at 1610–1630 cm^{-1}, and $\nu_{as\ O-C-O}$ at 1320–1340 cm^{-1}), and bicarbonate/hydrogen carbonate ($\nu_{as\ O-C-O}$ at 1650 cm^{-1}, and $\nu_{as\ O-C-O}$ at 1480 cm^{-1}). They are formed on high-strength basic sites (surface basic oxygen sites), medium-strength basic sites (surface basic oxygen sites) and low-strength basic sites (surface basic hydroxyl groups), respectively, as reported elsewhere [48]. Here, according to the stability of carbonate, the bands at 1681, 1650, 1359, and 1344 cm^{-1} are assigned to carbonate on low-strength basic sites, as they are less stable and their intensities dramatically decrease after subsequent evacuation; the bands at 1622, 1420, and 1380 cm^{-1} are assigned to carbonate on medium-strength basic sites, as they are medium stable; the band at 1480 cm^{-1} are assigned to carbonate on high-strength basic sites, as they are most stable and not influenced by evacuation. Obviously, after evacuation at high temperature (490 °C), the remained carbonate species on BaO-MCM-41N are more than that on BaO-MCM-41. It indicates that nitridation enhances the interaction of surface basic sites with adsorbed CO_2. In other words, nitridation increases the surface basic strength and/or forms new basic sites on the surface, in consistent with the XPS results.

Fig. 8 shows the IR spectra of CO_2 adsorbed on BaO-SBA-15 before and after nitridation. In the region of linear CO_2 adsorption (Fig. 8A), similar to BaO-MCM-41, bands at 2347, 2326, and 2280 cm^{-1} attributed to linear CO_2 adsorbed on Ba^{2+}, less exposed Ba^{2+}, and $^{13}CO_2$, respectively. After evacuation treatment, the dominated band does not split, which is different to BaO-MCM-41 and BaO-MCM-41N. Also, the interaction of CO_2 with Lewis acid sites is not strengthened by nitridation. In the region of carbonate-like species (Fig. 8B), same bands at 1686, 1652, 1620, 1466, 1405, 1382, and 1357 cm^{-1} are observed. According to the stability of species, the bands at 1686, 1652, and 1357 cm^{-1} are assigned to carbonate on low-strength basic sites, the bands at 1620, 1405, and 1382 cm^{-1} are assigned to carbonate on medium-strength basic sites, and the band at 1466 cm^{-1} is assigned to carbonate on high-strength basic sites. Compared to BaO-MCM-41 before and after nitridation, the carbonate species on BaO-SBA-15 before and after nitridation are

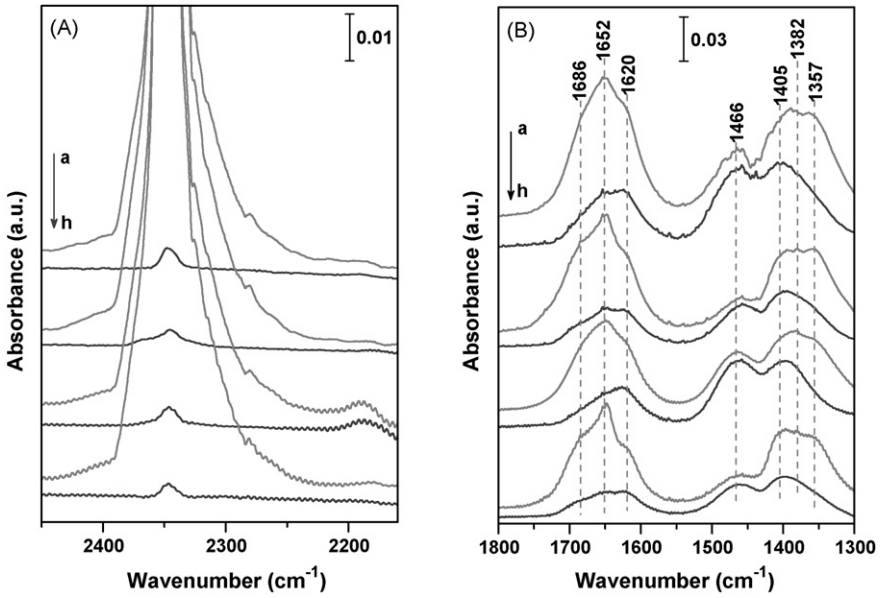

Fig. 8. IR spectra of (a) 21 hpa CO_2 on BaO-SBA-15 evacuated at 300 °C for 2 h, (b) following evacuated at RT for 1 h, (c) 20 hpa CO_2 on BaO-SBA-15 evacuated at 490 °C for 1 h, (d) following evacuated at RT for 1 h, (e) 21.3 hpa CO_2 on BaO-SBA-15N evacuated at 300 °C for 2 h, (f) following evacuated at RT for 1 h, (g) 21.3 hpa CO_2 on BaO-SBA-15N evacuated at 490 °C for 1 h, and (h) following evacuated at RT for 1 h.

much more stable. It suggests that the surface basicity of BaO-SBA-15/SBA-15N is stronger than that of BaO-MCM-41/MCM-41N. Also, the band at 1466 cm^{-1} increases after nitridation, indicating that the high-strength basic sites are improved by nitridation. This is also in consistent with the XPS results. Obviously, the nature of the surface basic sites on BaO-SBA-15 is very different with that on BaO-MCM-41, whatever before or after nitridation. A possible explanation may lie in the different surface and mesoporous structure of MCM-41 and SBA-15.

It should be noted that the bridging –NH– groups, the new basic sites formed by nitridation, may interact with CO_2 as hydroxyl groups. Then new carbonate-like specie would be formed, as shown in Scheme 1. However, no evidence about this new carbonate-like specie is obtained. A possible explanation is that the IR band corresponding to new carbonate-like specie may be overlapping by other carbonate species. Further researches on this are in progress.

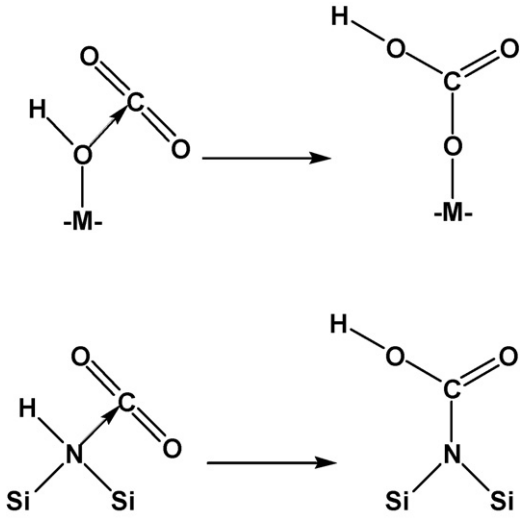

Scheme 1. Interaction of –OH groups ((1), from Ref. [45]) and bridging –NH– groups (2) with CO_2.

3.3. Catalytic results

3.3.1. Conversion of 2-propanol

The conversion of 2-propanol is one of the most popular model reaction for the characterization of acid and basic sites of catalysts. The 2-propanol decomposes through two parallel reactions: dehydration to propene mainly on acid sites, and dehydrogenation to acetone on basic sites. Here, the conversion of 2-propanol and the selectivity to acetone are employed to determine the basic property of BaO-MCM-41/SBA-15 before and after nitridation. The results of 2-propanol dehydrogenation on BaO-MCM-41/SBA-15 before and after nitridation are shown in Fig. 9. The only product is acetone and propene and no other product, like di-isopropyl ether is formed by the presence of the pairs of Lewis basic and acidic centers on the surface of catalysts [34,49], can be detected in the product. It can be seen that with increasing reaction temperature, the conversion of 2-propanol and selectivity to acetone increase. When the reaction temperature is below 500 °C, the conversion of 2-propanol on BaO-MCM-41/SBA-15 is higher than that on BaO-MCM-41N/SBA-15N, and the dehydration is the main reaction. However, when the reaction temperature is over 500 °C, the conversion of 2-propanol can nearly reach to 100% on BaO-MCM-41/SBA-15 both before and after nitridation. Meanwhile, dehydrogenation becomes the main reaction. The selectivity to acetone on BaO-MCM-41N and BaO-SBA-15N at 600 °C can reach up to 58.1% and 68.4%, respectively. The reason may be attributed to that the dehydrogenation requires higher active energy than the dehydration and can be greatly accelerated by the increase of reaction temperature. Obviously, the selectivity to acetone on BaO-MCM-41N/SBA-15N is always higher than that on BaO-MCM-41/SBA-15, indicating that the surface basicity of BaO-MCM-41N/SBA-15N is improved by nitridation.

A feature to note is that the selectivity to acetone on BaO-SBA-15N is higher than that on BaO-MCM-41N when reaction temperature is over 500 °C, due to the stronger basicity and/or more high-strength basic sites of the former than that of the latter. However, when the reaction temperature is below 500 °C, the selectivity to acetone on BaO-SBA-15N is much lower than that on BaO-MCM-41N. This may be originated from the different surface structure of BaO-MCM-41 and BaO-SBA-15 before and after nitridation.

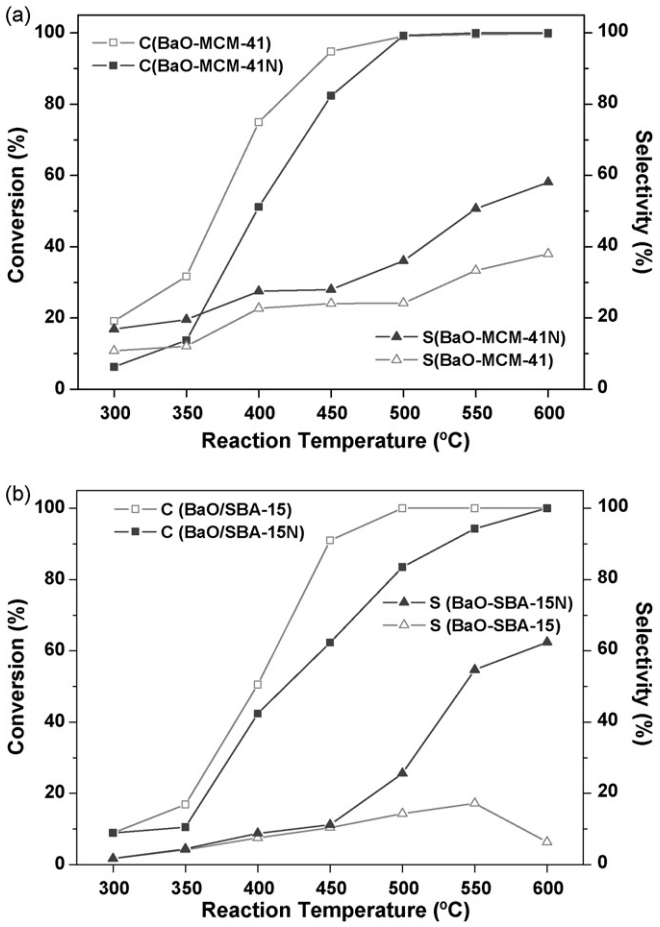

Fig. 9. Conversion of 2-propanol and selectivity to acetone over BaO-MCM-41 (a) and BaO-SBA-15 (b) before and after nitridation (reaction conditions: N_2 – 20 ml/min; isopropanol – 0.4 ml/h; catalyst – 0.2 g).

3.3.2. Knoevenagel condensation

The Knoevenagel condensation, which is a base catalysis reaction under mild conditions and is often considered as a typical basic probe reaction to evaluate the basic catalytic properties of nitrogen-incorporated zeolites [20,25,27,29] and mesoporous materials [13,17], is also adopted to explore the basic properties of as-prepared samples and the results are summarized in Table 3. Both MCM-41 and SBA-15 mesoporous supports show no activity in the Knoevenagel reaction, due to the absence of basic center on the surface. After loading of BaO, both BaO-MCM-41 and BaO-SBA-15 exhibit certain activity for Knoevenagel condensation. The conversion of benzaldehyde is 20.5% on BaO-MCM-41 and 75.2% on BaO-SBA-15 after reaction for 3 h. After nitridation, the basic catalytic activity of BaO-MCM-41/SBA-15 is further promoted. The conversion of benzaldehyde on BaO-MCM-41 and BaO-SBA-15 can reach up to 100% and 96.4% after reaction for 3 h, respectively. Obviously, the basic property of BaO-MCM-41/SBA-15 is greatly improved by nitridation, which is consistent with the result of basic characterization by XPS and IR. However, it was also found that the selectivity to benzylidene malononitrile was close to 100% for all samples and no further reaction such as the Michael addition reaction, which involves the reaction of benzylidene malononitrile with another malononitrile molecule and requires stronger basic sites than Knoevenagel condensation [50], can be detected. Besides BaO is not a good catalyst for Michael addition reaction, the low reaction temperature is also a key reason for Michael addition reaction and few products of Michael addition can be found when the reaction temperature is raised up to 90 °C. It can be also seen that the conversion of benzaldehyde on BaO-SBA-15 is much higher than that on BaO-MCM-41 in reaction 3 h. However, after nitridation, the basic catalytic activity of BaO-MCM-41N became higher than that of BaO-SBA-15N, although the surface basicity of the former is lower than that of the latter. The reason was suggested by Narasimharao et al. [29] that besides the basic sites, the nature of the surface species also plays an important role in effecting the catalytic activity of benzaldehyde and high catalytic activity for Knoevenagel condensations may requires both acidic and basic sites.

Table 3
Results of the Knoevenagel condensation over BaO-MCM-41/SBA-15 before and after nitridation.

Catalysts	Benzaldehyde conversion (%) at different reaction time (t)		
	t = 0.5 h	t = 2 h	t = 3 h
MCM-41	0	0	0
SBA-15	0	0	0
BaO-MCM-41	11.9	17.3	20.5
BaO-MCM-41N	70.3	99.2	100
BaO-SBA-15	33.4	50.8	75.2
BaO-SBA-15N	51.2	82.6	96.4

4. Conclusion

BaO loading forms surface basic species of Ba_2SiO_4 and $Ba_4Si_6O_{16}$ on MCM-41 and SBA-15, respectively. After nitridation, the former species are preserved and the latter species transform into Ba_2SiO_4 species. Demonstrated by XPS and adsorbed IR characterizations, the surface basic property of both BaO-MCM-41 and BaO-SBA-15 are improved, as bridging –NH– groups, another basic sites, are introduced into the framework of the mesoporous support by nitridation. Correspondingly, enhanced performances in base-catalyzed reactions, i.e. 2-propanol conversion to acetone and Knoevenagel condensation, can be obtained on BaO-MCM-41N/SBA-15N. Moreover, the surface basicity of BaO-SBA-15/SBA-15N is somewhat different to BaO-MCM-41/MCM-41N, which may be originated from their different surface and mesoporous structures. Unambiguously, nitridation can be used to modify the surface basic property. However, although the adsorbed IR characterizations indicate the improvement of surface basicity by nitridation, the results are far from satisfactory and the nature of each basic center is still missing. More suitable probe molecules are desiderated to be developed.

Acknowledgements

This work was financially supported by National Basic Research Program (No. 2009CB623502), National Natural Science Foundation of China (No. 20777039 and 20973094), and International S&T Cooperation Program of China (No. 2007DFA90720). We also greatly thank Dr. Mihail Mihaylov for the IR characterization.

References

[1] H. Hattori, Chem. Rev. 95 (1995) 537–558.
[2] T. Yashima, K. Sato, T. Hayasaka, N. Hara, J. Catal. 26 (1972) 303–312.
[3] A. Corma, S. Iborra, S. Miguel, Appl. Catal. 59 (1990) 237–248.
[4] A. Corma, S. Iborra, Adv. Catal. 49 (2006) 239–302.
[5] P.E. Hathaway, M.E. Davis, J. Catal. 116 (1989) 263–278.
[6] K.R. Kloetstra, H. van Bekkum, Chem. Commun. (1995) 1005–1006.
[7] L.R.M. Martens, P.J. Grobet, P.A. Jacobs, Nature 315 (1985) 568–570.
[8] A. Corma, R.M. Martin-Aranda, F. Sanchez, J. Catal. 126 (1990) 192–198.
[9] M. Laspéras, T. Liorett, L. Chaves, I. Rodrigues, A. Chauvel, D. Brunel, Stud. Surf. Sci. Catal. 108 (1997) 75–82.
[10] R. Sercheli, A.L.B. Ferreira, M.C. Guerreiro, R.M. Vargas, R.A. Sheldon, U. Schuchardt, Tetrahedron Lett. 38 (1997) 1325–1328.
[11] H. Yoshitake, T. Yokoi, T. Tatsumi, Chem. Mater. 14 (2002) 4603–4610.

[12] Y. Inaki, Y. Kajita, H. Yoshida, K. Ito, T. Hattori, Chem. Commun. (2001) 2358–2359.
[13] Y. Xia, R. Mokaya, Angew. Chem. Int. Ed. 42 (2003) 2639–2644.
[14] Y. Xia, R. Mokaya, J. Phys. Chem. C 112 (2008) 1455–1462.
[15] N. Chino, T. Okubo, Micropor. Mesopor. Mater. 87 (2005) 15–22.
[16] J. Wang, Q. Liu, Micropor. Mesopor. Mater. 83 (2005) 225–232.
[17] Y. Xia, R. Mokaya, J. Mater. Chem. 14 (2004) 2507–2515.
[18] C. Zhang, Q. Liu, Z. Xu, J. Non-Cryst. Solids 351 (2005) 1377–1382.
[19] G.T. Kerr, G.R. Shipman, J. Phys. Chem. 72 (1968) 3071–3072.
[20] S. Ernst, M. Hartmann, S. Sauerbeck, T. Brongers, Appl. Catal. A: Gen. 200 (2000) 117–123.
[21] K.D. Hammond, F. Dogan, G.A. Tompsett, V. Agarwal, W.C. Conner Jr., C.P. Grey, S.M. Auerbach, J. Am. Chem. Soc. 130 (2008) 14912–14913.
[22] F. Dogan, K.D. Hammond, G.A. Tompsett, H. Huo, W.C. Conner Jr., S.M. Auerbach, C.P. Grey, J. Am. Chem. Soc. 131 (2009) 11062–11079.
[23] K.D. Hammond, M. Gharibeh, G.A. Tompsett, F. Dogan, A.V. Brown, C.P. Grey, S.M. Auerbach, Wm.C. Conner Jr., Chem. Mater. 22 (2010) 130–142.
[24] J. Xiong, Y. Ding, H. Zhu, L. Yan, X. Liu, L. Lin, J. Phys. Chem. B 107 (2003) 1366–1369.
[25] C. Zhang, Z. Xu, K. Wan, Q. Liu, Appl. Catal. A: Gen. 258 (2004) 55–61.
[26] X. Guan, N. Li, G. Wu, J. Chen, F. Zhang, N. Guan, J. Mol. Catal. A: Chem. 248 (2006) 220–225.
[27] G. Wu, X. Wang, Y. Yang, L. Li, G. Wang, N. Guan, Micropor. Mesopor. Mater. 127 (2010) 25–31.
[28] X. Guan, F. Zhang, G. Wu, N. Guan, Mater. Lett. 60 (2006) 3141–3144.
[29] K. Narasimharao, M. Hartmann, H.H. Thiel, S. Ernst, Micropor. Mesopor. Mater. 90 (2006) 377–383.
[30] L. Regli, S. Bordiga, C. Busco, C. Prestipino, P. Ugliengo, A. Zecchina, C. Lamberti, J. Am. Chem. Soc. 129 (2007) 12131–12140.
[31] D. Lesthaeghe, V. Van Speybroeck, M. Waroquier, J. Am. Chem. Soc. 126 (2004) 9162–9163.
[32] D. Lesthaeghe, V. Van Speybroeck, C.B. Marin, M. Waroquier, J. Chem. Phys. B 109 (2005) 7952–7960.
[33] J. Weitkamp, M. Hunger, U. Rymsa, Micropor. Mesopor. Mater. 48 (2001) 255–270.
[34] V. Calvino-Casilda, R. Martin-Aranda, I. Sobczak, M. Ziolek, Appl. Catal. A: Gen. 303 (2006) 121–130.
[35] G. Busca, Chem. Rev. 110 (2010) 2217–2249.
[36] L. Liu, G. Zhang, J. Dong, Acta Phys. Chim. Sin. 20 (2004) 65–69.
[37] D. Zhao, Q. Huo, J. Feng, B.F. Chmelka, G.D. Stucky, J. Am. Chem. Soc. 120 (1998) 6024–6036.
[38] Q. Li, S.E. Brown, L.J. Broadbelt, J.-G. Zheng, N.Q. Wu, Micropor. Mesopor. Mater. 59 (2003) 105–111.
[39] G. Busca, V. Lorenzelli, G. Porcile, Mater. Chem. Phys. 14 (1986) 123–140.
[40] E. López-Salinas, M. García-Sánchez, Ma.E. Lianos-Serrano, J. Navarrete-Bolañoz, J. Phys. Chem. B 101 (1997) 5112–5117.
[41] H. Wiame, C. Cellier, P. Grange, J. Catal. 190 (2000) 406–418.
[42] E.A. Paukstis, N.S. Kotsarenko, L.G. Karakchiev, React. Kinet. Catal. Lett. 12 (1979) 315–319.
[43] E.A. Paukstis, E.N. Yurchenko, Russ. Chem. Rev. 52 (1983) 242–258.
[44] R. Astala, S.M. Auerbach, J. Am. Chem. Soc. 126 (2004) 1843–1848.
[45] J.C. Lavalley, Catal. Today 27 (1996) 377–401.
[46] G. Martra, R. Ocule, L. Marchese, G. Centi, S. Coluccia, Catal. Today 73 (2002) 83–93.
[47] B. Bonelli, B. Civalleri, B. Fubini, P. Ugliengo, C.O. Areán, E. Garrone, J. Phys. Chem. B 104 (2000) 10978–10988.
[48] J.I. Di Cosimo, V.K. Díez, M. Xu, E. Iglesia, C.R. Apesteguía, J. Catal. 178 (1998) 499–510.
[49] A. Gervasisni, J. Fenyvesi, A. Auroux, Catal. Lett. 43 (1997) 219–228.
[50] M.J. Climent, A. Corma, R. Guil-Lopez, S. Iborra, Catal. Lett. 74 (2001) 161–167.